Electronic Supplementary Material (ESI) for Lab on a Chip.

Supplementary Material

Microfluidics aided fabrication of 3D micro-nano hierarchical SERS substrate for rapid detection of dual hepatocellular carcinoma biomarkers

Changbiao Zhan, Zihao Guan, Liandong Yu,* Tongmei Jing, Huakun Jia, Xiaozhe Chen, Rongke Gao*

College of Control Science and Engineering, China University of Petroleum (East China), Qingdao 266580, China.

*** Address for correspondence:**

Rongke Gao

Telephone: +86-13023091659; E-mail addresses: rkgao@upc.edu.cn

Liandong Yu

E-mail addresses: liandongyu@upc.edu.cn

1. Experimental details

1.1 The details of calculating enhancement factor (EF)

According to the previous paper, 10^{-6} M MGITC solution was added to the optimized SERS substrate and slide glass. After natural air-drying procedure, we performed Raman detection to obtain normal Raman spectra and SERS spectra displayed in Figure S6d. N_{SERS} is the number of MGITC molecules covering the SERS substrate under the laser spot, and N_{bulk} refers to the number of MGITC molecules excited by the laser on the slide glass (Figure S11). S_{MGITC} was around 10^4 nm^2. Thus, the N_{SERS} was calculated to be $2.25*10^2$ following the equation (1). N_{bulk} was calculated through the equation (2). A was Avogadro constant (6×10^{23}), h was the laser penetration depth (3.48 μm), S was the area of laser spot (~ 2.25 μm^2), ρ_{MGITC} was the density of MGITC (1.31 g/cm^3), M_{MGITC} was molar mass of MGITC (485.98 g/mol). I_{SERS} and I_{bulk} were extracted from the spectra in Figure S6d. EF was calculated to be 1.5×10^8 through the equation (3)

$$N_{SERS} = \frac{S_{laser}}{S_{MGITC}} \#(1)$$

$$N_{bulk} = \frac{A \times (S \times h \times \rho_{MGITC})}{M_{MGITC}} \#(2)$$

$$EF = \frac{I_{SERS}}{I_{bulk}} \times \frac{N_{bulk}}{N_{SERS}} \#(3)$$

1.2. Materials

Hexadecane, Poly (ethylene glycol) diacrylate (PEGDA, Mn 700), Gold (III) chloride trihydrate ($HAuCl_4 \bullet 3H_2O$, >99.9%), sodium citrate dehydrate (99%), bovine serum albumin (BSA), Span 80 nonionic surfactant, Malachite green isothiocyanate (MGITC) and 3,3′-diethylthiadicarbocyanine iodide (DTDC), alpha-L-Fucosidase (AFU) and monoclonal antibody (McAb) to AFU were purchased from Sigma-Aldrich. Human Alpha fetoprotein (AFP), human AFP monoclonal antibody (Ab1), Mouse anti human AFP monoclonal antibody (Ab2) were obtained from Shanghai Linc-Bio Science Co, Ltd. (Shanghai, China). Photoinitiator (Omnirad 2959) was purchased from Thunder Chemical Shanghai, Ltd. Phosphate-buffered saline (PBS) solutions were obtained from Sangon Biotech (Shanghai, China).

1.3. Preparation of AFP/AFU detection antibody-conjugated AuNPs

The preparation of functionalized AuNPs has been reported in our previous work.[1] In brief, DTDC solution was dropped in 1 mL of a 0.1 nM AuNPs solution and placed in a vortex shaker for 30 min. Then, 100 μL of 0.1 M boric acid buffer and add 2 μL of 0.1 mg mL^{-1} AFP detection antibody were serially added into the mixture for 2 h reaction with stirring. 20 μL of 10% (m/m) BSA was employed to deactivate unreacted sites on the surface of the AuNPs for 30 minutes. The antibody-conjugated AuNPs were stored in 4°C refrigerator to stabilize for 1 hour. Finally, the non-specific binders were washed three times with deionized water. The modification process of AFU detection antibody was the same as that of AFP (Figure S5a).

1.4. Instruments

The excitation source of Raman microscope system was a He-Ne laser with a power of 5 mW and an operating wavelength of 632.8 nm. The laser spot size after 30% ND filtering is close to 1.5 μm with a 50× objective (0.5 NA). The accumulation number and exposure time for each point were 3 and 10 s. A 60 μm (x-axis) by 60 μm (y-axis) range under computer control yielded rectangular Raman mapping images with 400 pixels (1 pixel ≈ 3 μm × 3 μm). The accumulation number and exposure time for each pixel were 1 and 1 s, respectively. The absorption spectra were obtained with Cary 5000 UV–vis-NIR spectrophotometer (Agilent Technologies, Inc., USA) with an integrating sphere detector unit. In order to control the experimental variables, the samples were dropped on a PET film with a side length of 2 cm, and then covered with another clean PET film of the same size. Scanning electron microscope (SEM) images of the substrate was carried out through a Hitachi-SU8020 (Hitachi, Japan). All samples can be dried at room temperature.

1.5. The amount of capture antibodies per SAHM

Regarding the number of antibodies (Abs) per microparticle, it is determined by mass difference between the antibodies added to a suspension of SAHMs and the unbound antibodies remaining in the supernatant when separated from the formed Abs−SAHMs conjugates.[2] The peptide bonds of proteins have strong UV absorption at 200-250 nm. In order to evaluate the amount of functional capture antibodies per SAHMs, we quantified the change of antibody concentration in solution before and after antibody modification by measuring the absorbance at 200-250 nm as shown in Figure S10. The formula of Lambert-Beer law was as follow:

$$A = \varepsilon bc$$

A is the absorbance, ε is the molar absorption coefficient, c is optical path length. The number of SAHMs used to modify antibodies is approximately 7000 mL^{-1}. Thus, the amount of functional capture antibody per SAHM was calculated to be approximately 0.91 ng.

2. Figures

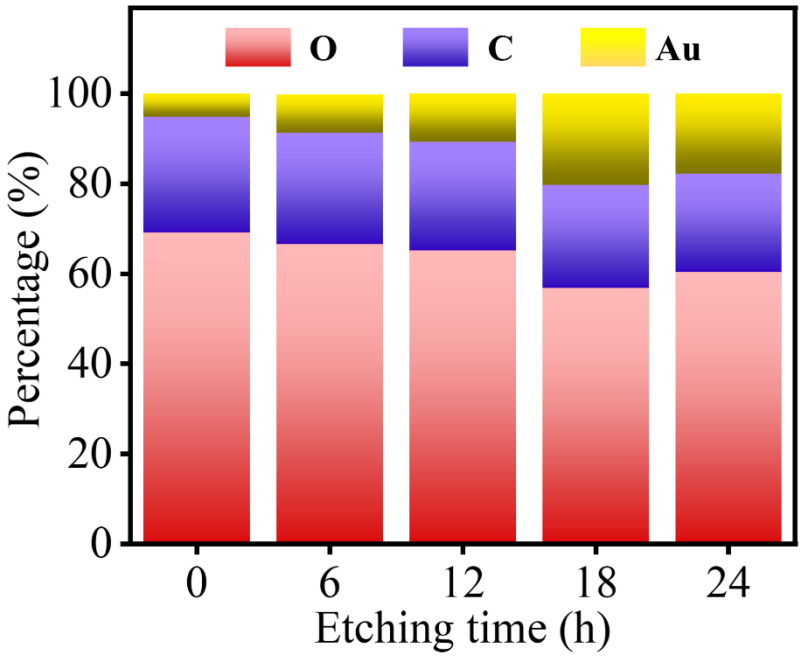

Figure S1. The amount of Au loading on SAHMs varied as a function of the etching time.

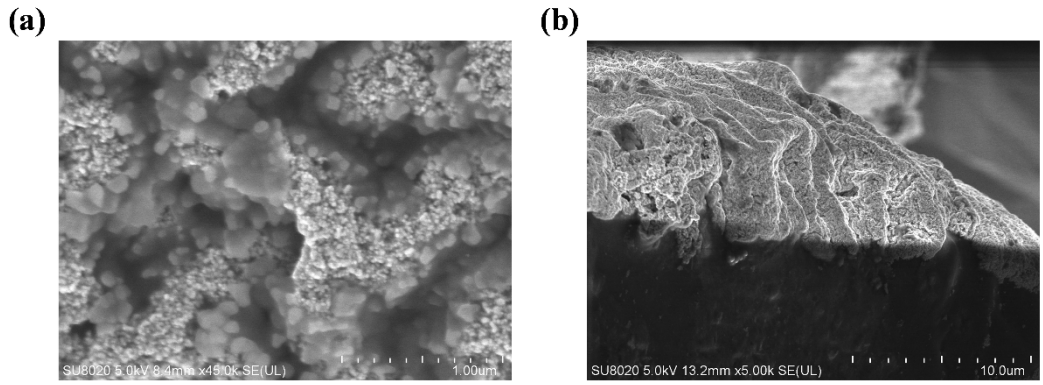

Figure S2. The top view (a) and side view (b) of the wrinkle structures.

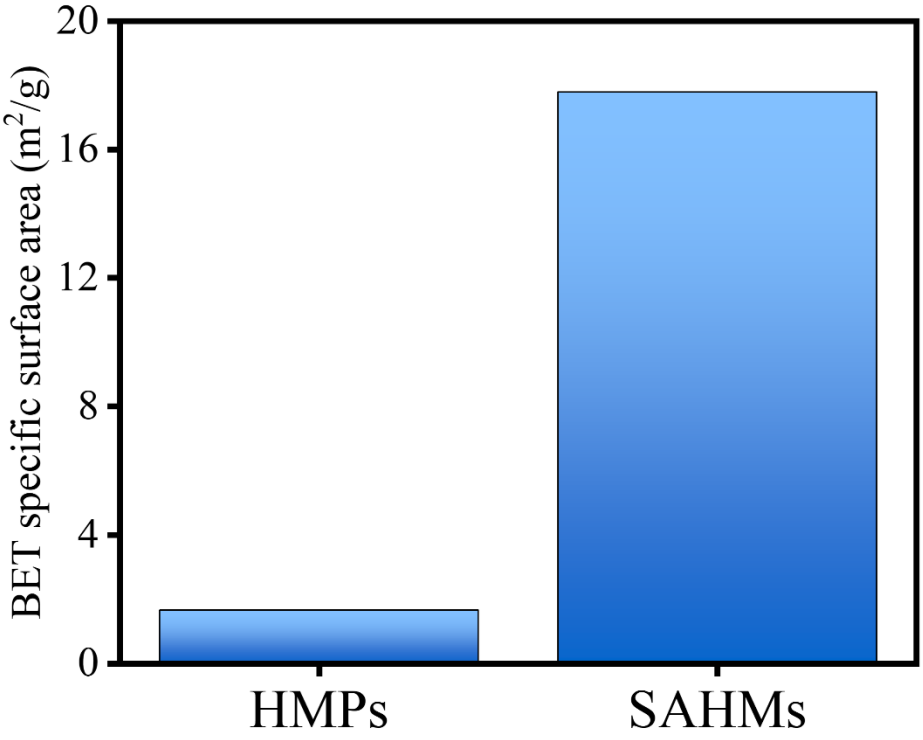

Figure S3. The BET specific surface area of HMPs and SAHMs.

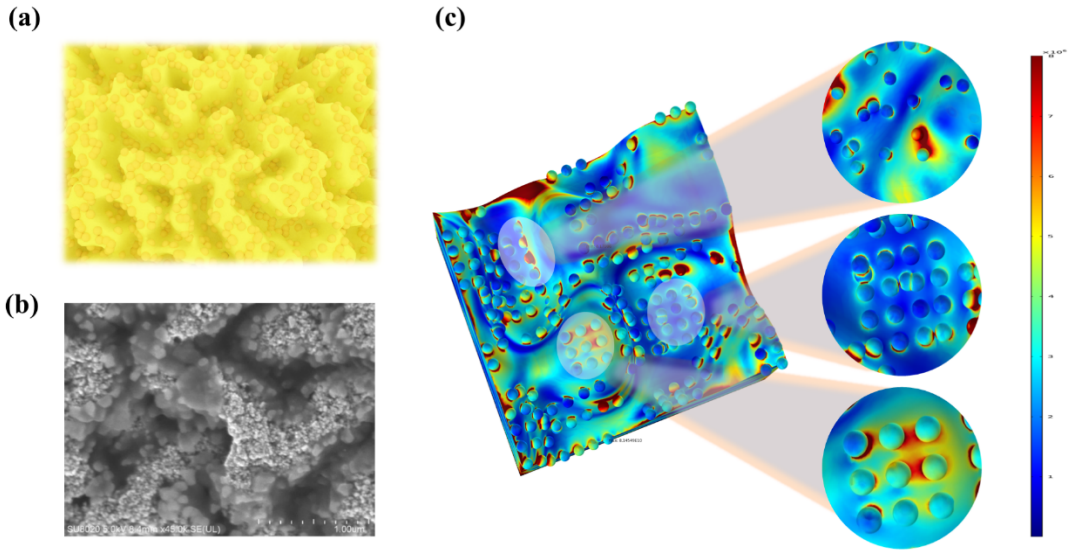

Figure S4. (a-b) Schematic and SEM image of the SAHMs. (c) COMSOL simulation of the electric field distribution on the SAHMs.

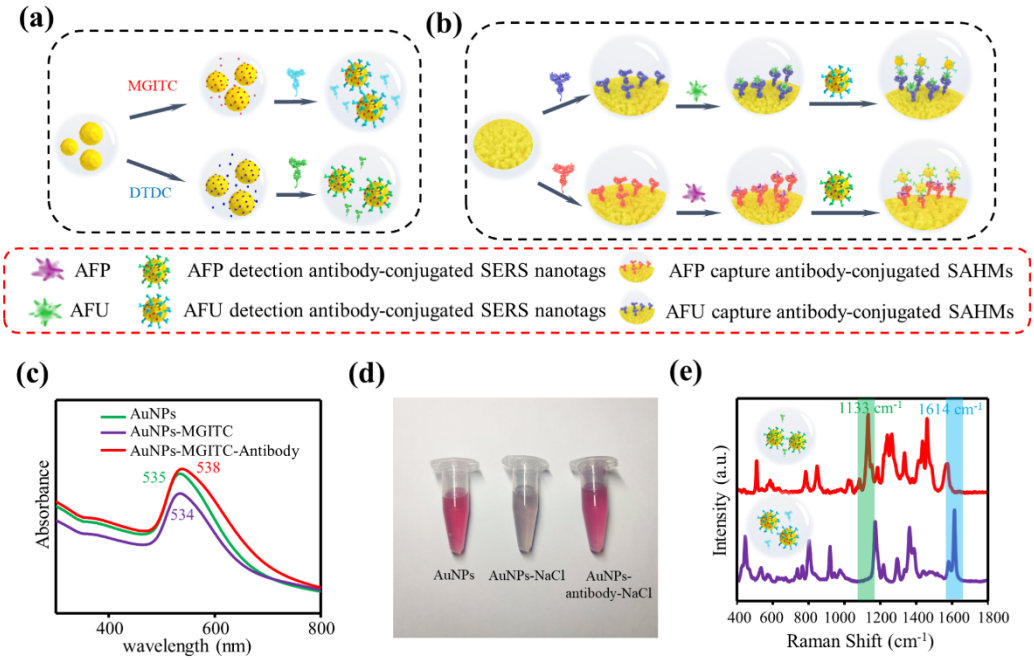

Figure S5. (a) Sequential process for preparing two different types of antibody-conjugated SERS nanotags. (b) Preparation steps of "sandwich" immunocomplexes on SAHMs. (c) The UV−vis absorption spectra for AuNPs and SERS nanotags with detection antibodies. (d) The photograph of salt aging experiments. (e) SERS spectra of two individual nanotags (DTDC and MGITC).

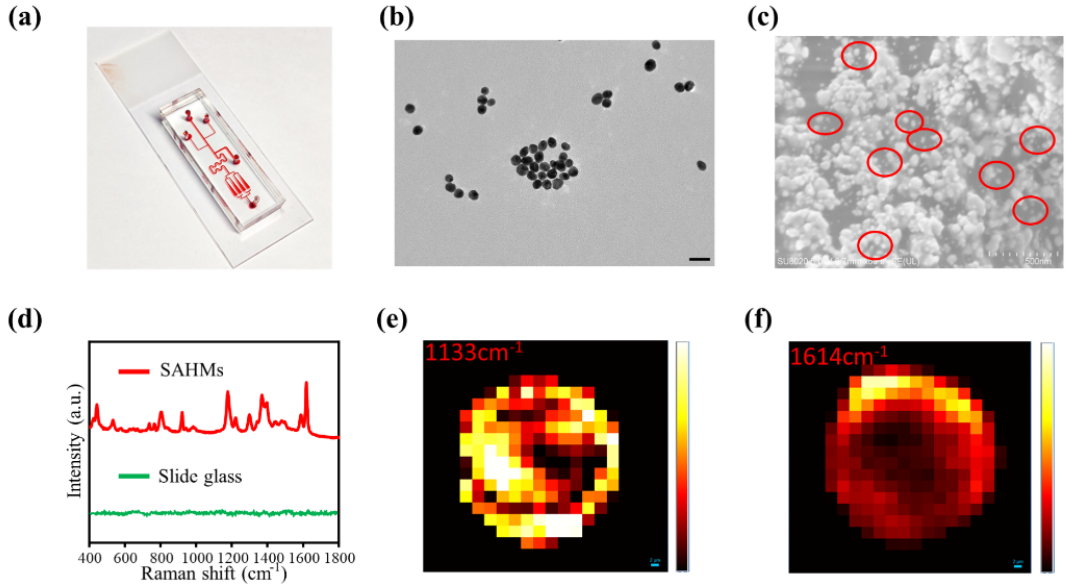

Figure S6. (a) The photograph of the microfluidic chip for SERS detection containing red ink. (b) The representative TEM image of AuNPs. The scale bar is 100 nm. (c) SEM image of the SERS nanotags distributed on the SAHMs by immunocomplexes. (d) The SERS spectrum of 10-6 M MGITC on the SAHMs and its normal Raman spectrum on slide glass. (e-f) SERS mapping images of immunocomplexes obtained from the SAHMs with 50 ng mL^{-1} of AFP and AFU. The scale bar is 2 μm.

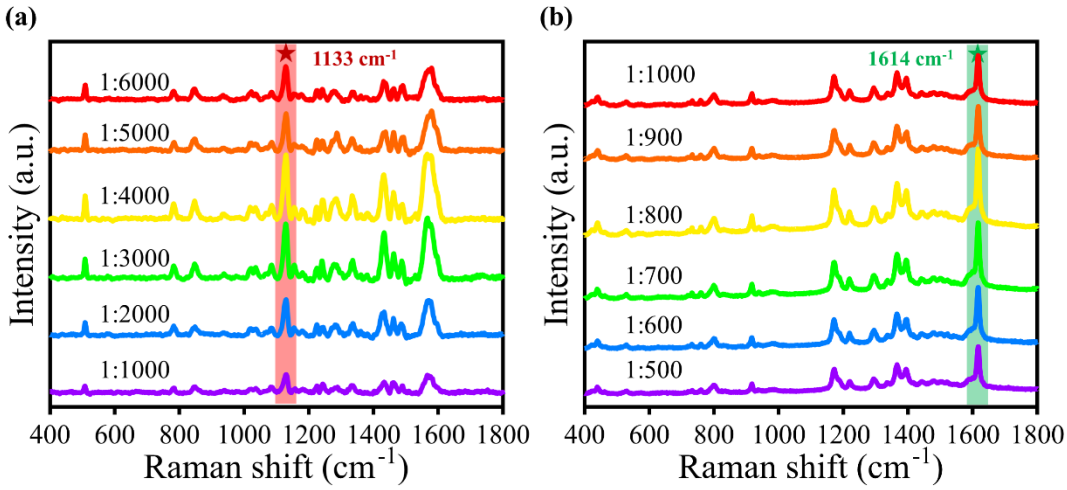

Figure S7. SERS spectra of the nanotags with different ratios of AuNPs to reporter molecules DTDC (a) and MGITC (b).

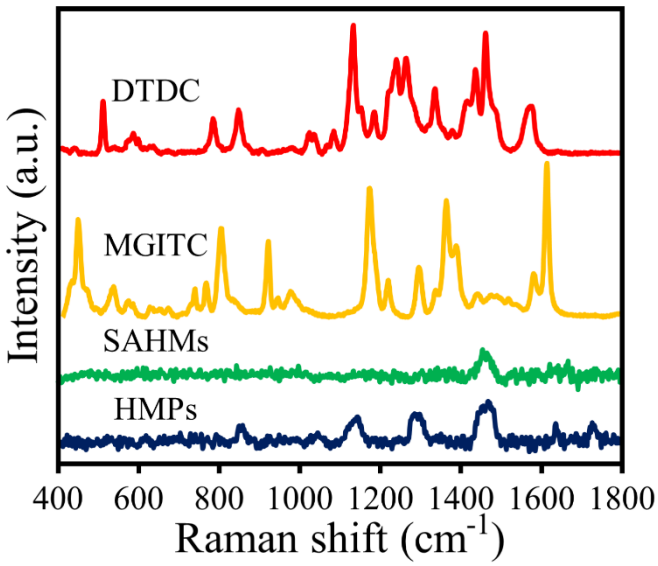

Figure S8. Raman spectra of the HMPs, SAHMs, MGITC, and DTDC.

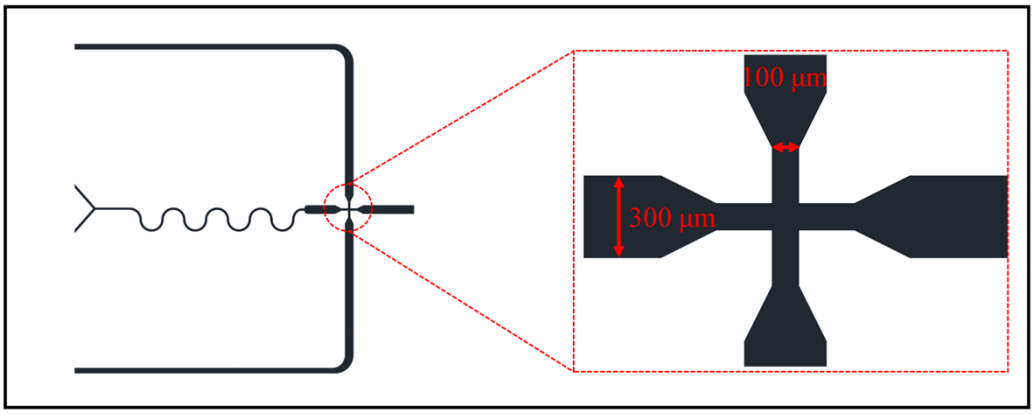

Figure S9. The CAD design of the microdroplet generation unit.

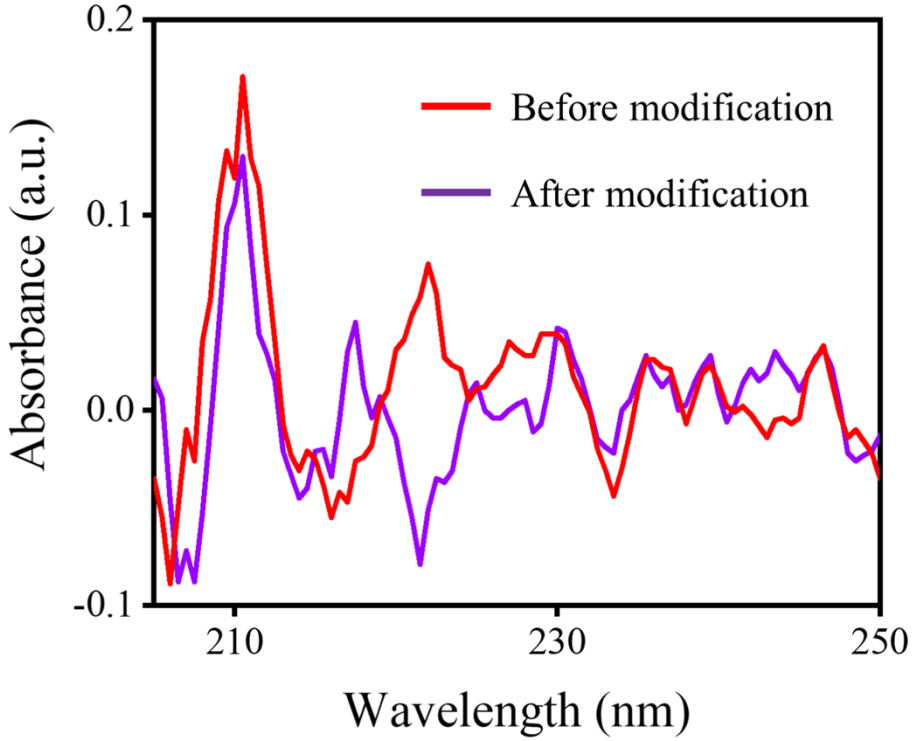

Figure S10. The UV absorbance at 200-250 nm of antibody solution before and after modification on the SAHMs.

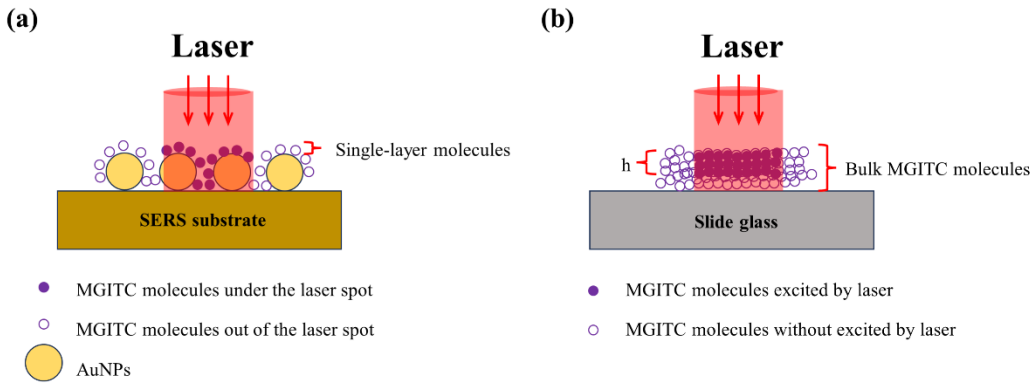

Figure S11. Schematic diagrams of N_{SERS} (a) and N_{bluk} (b).

Table S1. Vibrational assignments for the characteristic SERS peaks of DTDC, MGITC and HMPs (PEGDA).

DTDC Bands (cm^{-1})	**Assignment**
780	stretching of central carbon chain
847	C-H out-of-plane vibrations
1133	Raman skeletal optical mode A_g vibrational modes of all-*trans* rotamers
1153	C-C stretch in conjugated C=C molecules
1266	=C-H in-plane deformation, unconjugated
1438	CH_2 bend
1464	ring vibrations
1575	C=C stretching
MGITC Bands (cm^{-1})	**Assignment**
757	NH_2 bending, torsion
796	C-H bending from benzene ring
916	b_{1u} in plane benzene ring
1170	ν_9 benzene in plane
1218	N-C stretch + NR_2 bending
1295	In plane C-H and C-C-H
1363	N-Phenyl ring stretching
1391	In plane C-C and C-H
1586	In plane ring, stretch + bending
1614	N-Phenyl ring + C-C stretching
HMPs Bands (cm^{-1})	**Assignment**
858	Alicyclic chain vibrations
1285	=C-H in-plane deformation
1467	O-CH_2 deformation
1635	C=C stretching
1726	stretching of C=O

Table S2. The description of all acronym presented in manuscript.

Acronym	Description
HCC	Hepatocellular carcinoma
SERS	Surface-enhanced Raman scattering
SAHMs	SERS-active hydrogel microparticles
AuNPs	gold nanoparticles
AFP	alpha-fetoprotein
AFU	alpha-l-fucosidase
FLISA	Fluorescence immunosorbent assay
NMNPs	Noble metal nanoparticles
F-NPs	Ferro-nanoparticles
HMPs	hydrogel microparticles
AgNPs	Silver nanoparticles
PDMS	Polydimethylsiloxane
MGITC	Malachite green isothiocyanate
DTDC	3,3′-diethylthiadicarbocyanine iodide
PBS	Phosphate-buffered saline
McAb	monoclonal antibody
BSA	bovine serum albumin
PEGDA	polyethylene glycol diacrylate
SEM	scanning electron microscope
EF	enhancement factor
TEM	Transmission electron microscope
LOD	limit of detection

Table S3. Comparison of the proposed method for AFP and AFU with other reported works.

Analyst	Detection Method	Amplification Strategy	Detection Range	Detection Mode	Selectivity	Operation Mode	Reaction Time	Ref
AFP	SERS	Ag@aUNCs/ MoS_2	1 pg mL^{-1} -10 ng mL^{-1}	Singlet	N/A	Manual	2 h 5 min	[3]
	Electrochemical	HAP NPs	0.01-10 ng mL^{-1}	Singlet	HSA, CEA, GSH, IgG	Manual	1 h 50 min	[4]
	Photoelectrochemical	CdS-QDs	0.1-500 ng mL^{-1}	Singlet	CEA, PSA, H_2O_2	Manual	N/A	[5]
	Fluorescence	QDs- AuNPs	0.5-45 ng mL^{-1}	Singlet	BSA, CEA, HAS, IgG	Automatic	1 h 20 min	[6]
	Photoelectrochemical	MoS_2/Au/GaN	1.0-150 ng mL^{-1}	Singlet	CEA, TB, BSA	Manual	54 min	[7]
	Magnetoresistance	MBs	100 fg mL^{-1} μg mL^{-1}	Singlet	BSA, PSA	Automatic	5 h 30 min	[8]
	SERS-Microfluidics	SAHMs/ AuNPs	0.1-100 ng mL^{-1}	Multiple	AFU, BSA, PSA, Thrombin	Automatic	1 h 40 min	This work
AFU	Plasmonic	AuNPs	0.015-100 ng mL^{-1}	Multiple	N/A	Automatic	N/A	[9]
	Fluorescence	Carbon dots	3.8-67 ng mL^{-1}	Singlet	N/A	Manual	1 h 20 min	[10]
	Fluorescence	Polymer dots	0.01-0.9 ng mL^{-1}	Singlet	BSA, Leu, et al	Manual	20 min	[11]
	Quartz slide assay	Quartz	N/A	Singlet	BSA, HSA, IgG	Manual	2h 40 min	[12]
	SERS-Microfluidics	SAHMs/ AuNPs	0.01-10 ng mL^{-1}	Multiple	AFP, AFU, BSA, PSA	Automatic	1 h 40 min	This work

References

1. R. Gao, C. Zhan, C. Wu, Y. Lu, B. Cao, J. Huang, F. Wang and L. Yu, *Lab Chip*, 2021, DOI: 10.1039/d1lc00516b.
2. G. Ruiz, K. Tripathi, S. Okyem and J. D. Driskell, *Bioconjugate Chemistry*, 2019, **30**, 1182-1191.
3. E. Er, A. Sanchez-Iglesias, A. Silvestri, B. Arnaiz, L. M. Liz-Marzan, M. Prato and A. Criado, *ACS Appl Mater Interfaces*, 2021, **13**, 8823-8831.
4. J. Sun, D. Tian, Q. Guo, L. Zhang, W. Jiang and M. Yang, *Analytical Methods*, 2016, **8**, 7319-7323.
5. R. Xu, Y. Jiang, L. Xia, T. Zhang, L. Xu, S. Zhang, D. Liu and H. Song, *Biosens Bioelectron*, 2015, **74**, 411-417.
6. L. Zhou, F. Ji, T. Zhang, F. Wang, Y. Li, Z. Yu, X. Jin and B. Ruan, *Talanta*, 2019, **197**, 444-450.
7. D. Hu, H. Cui, X. Wang, F. Luo, B. Qiu, W. Cai, H. Huang, J. Wang and Z. Lin, *Anal Chem*, 2021, **93**, 7341-7347.
8. Y. Zhu, Q. Zhang, X. Li, H. Pan, J. Wang and Z. Zhao, *Sensors and Actuators B: Chemical*, 2019, **293**, 53-58.
9. X. Han, H. Shokri Kojori, R. M. Leblanc and S. J. Kim, *Anal Chem*, 2018, **90**, 7795-7799.
10. K. Mintz, E. Waidely, Y. Zhou, Z. Peng, A. O. Al-Youbi, A. S. Bashammakh, M. S. El-Shahawi and R. M. Leblanc, *Anal Chim Acta*, 2018, **1041**, 114-121.
11. X. Cheng, Y. Huang, D. Li, C. Yuan, Z.-L. Li, L. Sun, H. Jiang and J. Ma, *Sensors and Actuators B: Chemical*, 2019, **288**, 38-43.
12. E. Waidely, A. O. Al-Youbi, A. S. Bashammakh, M. S. El-Shahawi and R. M. Leblanc, *Anal Chem*, 2017, **89**, 9459-9466.